

RCS Validation of Asymptotic Techniques Using Measured Data of an Electrically Large Complex Model Airframe

Ciara Pienaar¹, Johann W. Odendaal¹, Johan Joubert¹, Johan C. Smit²,
and Jacques E. Cilliers²

¹ Department of Electrical Electronic and Computer Engineering
University of Pretoria, Pretoria, South Africa
u11175070@tuks.co.za, wimpie@up.ac.za, jjoubert@up.ac.za

² Defence Peace Safety and Security
Council for Scientific and Industrial Research, Pretoria, South Africa
jesmit@csir.co.za, jcilliers@csir.co.za

Abstract — This paper validates the accuracy with which various asymptotic techniques including RL-GO and SBR can calculate the RCS of an electrically large complex airframe. This target has a maximum electrical length of 106λ . Two CEM packages are utilized namely, CST MWS and FEKO. The simulated RCS results are compared to measured RCS data, obtained in a compact range. The effect of the 3D CAD model accuracy on the simulation accuracy is also investigated. Comparisons between simulated and measured RCS data are provided using RCS plots and ISAR images.

Index Terms — Asymptotic methods, CAD model accuracy, RCS measurements, validation.

I. INTRODUCTION

Radar cross section (RCS) modelling and simulation has a wide range of applications in the field of radar and electronic warfare (EW). These include platform detectability analysis, the generation of test data for development and testing of radar and EW systems, as well as signature database generation for applications such as non-cooperative target recognition (NCTR). For these applications it is important that calculated radar signatures of targets are accurate and obtained within reasonable timeframes. The accuracy of calculated RCS results depends on a few factors. Two of the factors, investigated in this study, include the accuracy of the 3-dimensional (3D) computer aided design (CAD) model of the target, as well as the computational electromagnetic (CEM) method utilized.

It was shown in [1] that the overall shape of targets CAD models, as well as small geometric features on the models can have an impact on the RCS scattering characteristics. The differences between four aircraft CAD models were investigated using simulated data and quantified using different contour-based shape

descriptors. The four targets included a Pilatus PC-21, an F-16 fighter jet, and two models of the same aircraft, namely a Cessna 172.

The second factor contributing to the simulation accuracy is the CEM method. Asymptotic CEM techniques are generally used for RCS predictions of electrically large complex targets. Numerous asymptotic techniques are available, which are capable of solving electrically large scattering problems within timeframes that are a fraction of the time required by full-wave methods. Some of these methods include physical optics (PO), geometrical optics (GO), the physical theory of diffraction (PTD), ray-launching GO (RL-GO), as well as shooting and bouncing rays (SBR).

In [2], a new efficient ray-tracing algorithm for the calculation of RCS, based on PO and PTD, was presented. This method was evaluated by comparing the monostatic RCS simulations of a few different targets, with either full-wave method of moments (MoM) results or RCS measurements used as reference. The targets investigated included a thin and thick flat plate, trihedral corner reflector, generic cruise missile and two aircraft models. The RCS results obtained for the first four targets were compared to MoM simulation results. Good agreements between the results were observed. The first aircraft target was a 1:32 scaled model with an electrical length of 60λ . The simulated results for this aircraft were compared to measured RCS data, with rather good agreement observed. The physical model used in the RCS measurements was manufactured using the simulated CAD model. High range resolution (HRR) profiles of both aircraft targets, scaled to original size, were generated using the data calculated with the PO and PTD algorithm, and compared to one another. It was observed that the objects could be distinguished based on these profiles.

Recently a study evaluated the suitability of three

CEM techniques, including the multilevel fast multipole method (MLFMM), PO and PO with SBR, for RCS calculations of electrically large targets [3]. Three targets were used for the analyses, and included a trihedral corner reflector, generic cruise missile similar to that used in [2], and the high fidelity Cessna 172 model used in [1]. Only simulated RCS results were considered, with MLFMM data used as reference for the comparisons. It was shown that the RCS of the corner reflector and generic cruise missile calculated with the PO and PO with SBR methods compared well with the MLFMM results.

In [4], the measured and simulated RCS data of a Boeing 777 scale model, with electrical length of 20λ , was compared. A commercially available 3D CAD model of the aircraft was simulated using the CADRCS software package. This package implements PO combined with ray-tracing and shadowing to calculate the RCS of objects. Although good correspondence between the main features in the RCS diagrams were obtained, differences were still observed which highlighted the need for different techniques to fully represent the RCS of an object.

In [5], the accuracy and efficiency with which full-wave and asymptotic CEM methods could predict the RCS of a large complex airframe was investigated. This study utilized the same physical 1:25 scale model of a Boeing 707 that was used in an installed antenna performance investigation [6]. RCS measurements of this target were obtained in a compact range at the University of Pretoria, South Africa. The methods that were validated included PO, PO with SBR and MLFMM. Three EM simulation packages were utilized in this study, viz. CST Microwave Studio (MWS), FEKO and SigmaHat. All of the methods showed good agreement with the measured data over the important azimuth ranges where the main features were found.

This paper serves to illustrate the effects of different options and asymptotic technique implementations on the simulated RCS results for a realistic representation of a large and complex model airframe. Measured RCS data of a conducting Boeing 707 scale model, with an electrical length of 106λ , is used to illustrate the effect of the geometrical accuracy of CAD models on calculated RCS results. Simulated data of a generic CAD model, constructed from canonical structures [6], and a laser scanned CAD model, generated from the physical airframe, are compared to the measured RCS results obtained in a compact range. Secondly, the accuracies of a few different implementations of asymptotic techniques to calculate the RCS of the large complex airframe are validated against the measured results. The methods include RL-GO as implemented in FEKO [7] and SBR using CST [8]. For the RL-GO method the effect of using different mesh types, consisting of linear and curvilinear triangles, is illustrated. The differences

between the measured and simulated RCS results using the SBR method with rays and ray-tubes are also presented. Comparisons of the measured and simulated datasets are conducted using RCS graphs and inverse synthetic aperture radar (ISAR) images to gain more insight into the scattering mechanisms.

II. CAD MODEL ACCURACY

RCS measurements of the scale model Boeing 707 were conducted in the compact range at the University of Pretoria, South Africa. This setup is shown in Fig. 1. An investigation of the effect of the geometrical accuracy of two different 3D CAD models of the target, on the simulation accuracy, was conducted. These models included the scanned and generic CAD models.



Fig. 1. Scale model setup in the compact range at the University of Pretoria, South Africa.

The scanned model was developed by converting the 3D point cloud, generated with a handheld laser scanner, to a mesh model using 3D processing software [5]. The mesh model was imported into FEKO where a simulation mesh was created. The scanned model has an average accuracy of better than 0.2 mm relative to the actual scale model. An overlay of these two models, with a zoomed in view of the engines, is provided in Fig. 2. The scanned CAD model is shown in yellow and the generic CAD model in orange.



Fig. 2. Overlay of scanned (yellow) and generic (orange) CAD models and zoomed-in view of engines.

The geometrical differences between the two CAD models are clearly observed in Fig. 2. The largest discrepancies are the wing alignments, the engine positions and the details within the engines. It can further be observed that the scanned CAD model is a more realistic and accurate representation of the actual scale model of the target that was used for the measurements, shown in Fig. 1.

Experiments were conducted to determine which CAD model of the target would be the preeminent model for validating the asymptotic methods. It was shown in [5] that the RCS of the Boeing 707, calculated with PO compared very well with the RCS calculated with the full-wave MLFMM method at 10 GHz and 17 GHz. Consequently it was decided to analyze the effect of the geometrical accuracy of the two CAD models, relative to the scale model, on the simulation accuracy with the PO method implemented in FEKO, at both these frequencies as well as at a lower frequency of 3 GHz. Figures 3, 4 and 5 provides a comparison between the measured data and PO simulated data generated with the scanned and generic CAD models at 3 GHz, 10 GHz and 17 GHz, respectively.

The PO simulations of both the scanned and generic CAD models produced comparable results to the measured data as seen in Figs. 3, 4 and 5. Larger discrepancies between both PO simulated data sets and the measured data are observed over 40° and 60° . It is however clear that, the scanned CAD model yields overall more accurate RCS results compared to the measured data than the results obtained with the generic CAD model. This is particularly evident in the nose (0°) and tail (180°) regions of the airplane where the RCS values are lower. As the frequency increases, the smaller details on the models play larger roles in the RCS signatures.

Further analyses of the structural behavior of the scale model and the scattering centers of the two CAD models were conducted. This was done by generating ISAR images of the measured and PO simulated targets that were illuminated from the front (-30° to 30°) and from the port broadside (60° to 120°). The ISAR measurements and simulations were conducted for VV-polarized monostatic RCS centered at 10 GHz using 801 frequencies in steps of 8 MHz, and 101 frequencies in steps of 60 MHz, respectively. Figures 6 and 7 provides the ISAR images of the physical scale model measured in the compact range and the PO simulation of the 3D scanned CAD model as well as the generic 3D CAD model illuminated from the front and side, respectively.

It is evident from the ISAR image of the measured data in Fig. 6 (a) that there are certain areas on the target that produce dominant scattering when illuminated in this range, such as the engines. The wings and nose of the aircraft also produce some scattering. Even though the wooden mounting rod used to position the model in the compact range was covered with radar absorbing material (RAM), it still produces some scattering, not present in the simulations. Almost no scattering is observed on the stabilizers of the aircraft. Very similar scattering patterns located at the nose and cockpit area of the measured scale model and scanned CAD model are observed in Figs. 6 (a) and (b). A

different scattering pattern is observed in this area of the generic CAD model seen in Fig. 6 (c). A lot less scattering is observed from the wings of the generic CAD model than with the measured data. Although the scattering produced by the engines of the scanned CAD model is slightly less than that of the physical scale model, these scattering patterns are very similar. The cavities in the engines of the generic CAD model produce slightly different scattering patterns than the enclosed engines of the scale model and scanned CAD model.

It is clear in Fig. 7 that the main parts contributing to the RCS of the aircraft, in this range, include the two visible port side engines, the fuselage, and the vertical stabilizer. The scattering produced by the fuselage of the CAD models are very similar to the measured data, however slightly less scattering is produced by the fuselage of the generic CAD model, Fig. 7 (c). The scattering center located on the vertical stabilizer of the generic CAD model is larger than that of the measured data. The obscured starboard side engines of the scale model and the scanned CAD model also contribute somewhat to the RCS patterns observed in Figs. 3, 4 and 5, whereas no scattering is observed from this part of the generic CAD model. The wingtip and the tip of the horizontal stabilizer of the scale model and the scanned CAD model produce scattering not observed with the generic CAD model.

The differences between the measured and simulated scattering centers observed in the ISAR images in Fig. 6 and Fig. 7, clarifies some of the discrepancies observed in the angular RCS data provided in Figs. 3, 4 and 5. It is evident that the scanned CAD model delivers more accurate scattering results compared to the measured data when comparing the various scattering centers. This can be attributed to the fact that the scanned CAD model is a more accurate geometrical representation of the actual scale model used for measurements than the generic CAD model. Additional scattering analysis of the scanned CAD model was therefore conducted to investigate the reason for the discrepancies observed between 40° and 60° . The ISAR images of measured and simulated data illuminated from 30° to 60° are provided in Figs. 8 (a) and (b).

A few main scattering points are observed in the image of the measured data, Fig. 8 (a). These are found at the leading edge of the wing, the juncture between the wing and the fuselage, the engines and the leading edge of the horizontal stabilizer of the aircraft. The corner reflector created between the wing and the fuselage is the dominant scattering center over this azimuth range. Some of the same scattering centers, although with lower intensity, are observed in the simulated data in Fig. 8 (b). The dominant measured scattering center located at the corner reflector, formed between the wing and the fuselage of the airplane, is

not present in the PO simulated data. This explains why the simulated RCS is lower than the measured data over this range.

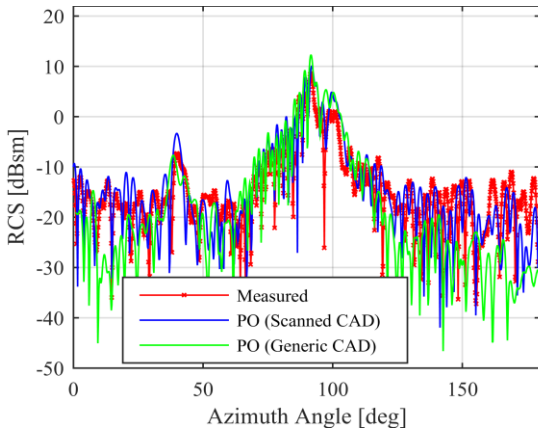


Fig. 3. RCS at 3 GHz measured and simulated in FEKO with PO using the scanned and generic CAD models.

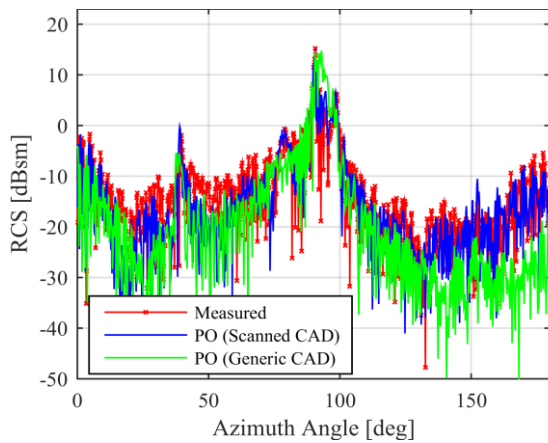


Fig. 4. RCS at 10 GHz measured and simulated in FEKO with PO using the scanned and generic CAD models.

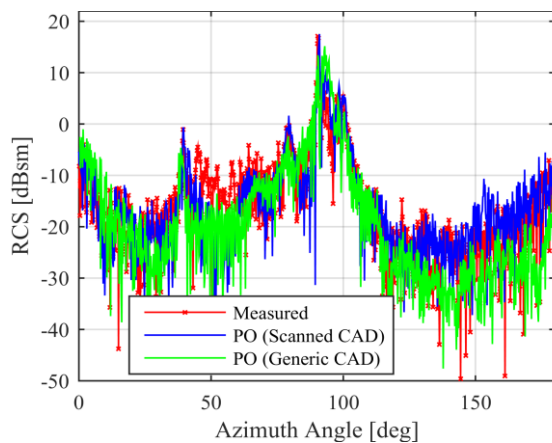


Fig. 5. RCS at 17 GHz measured and simulated in FEKO with PO using the scanned and generic CAD models.

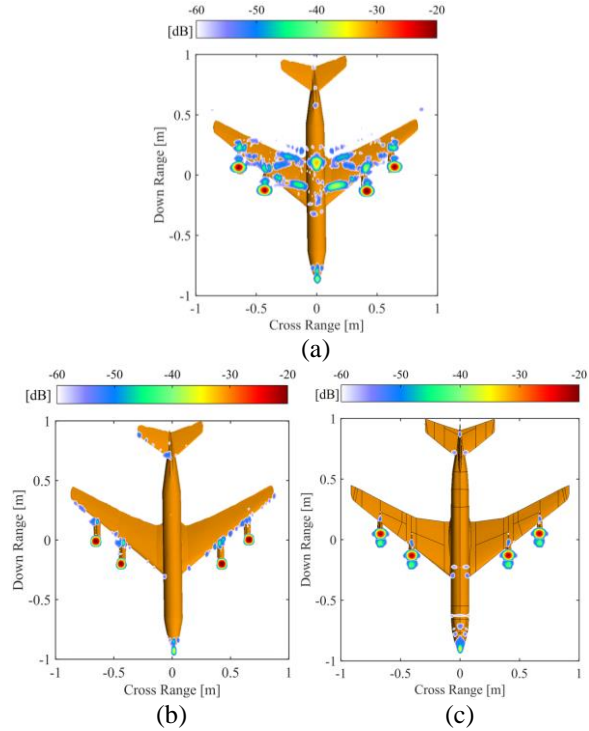


Fig. 6. ISAR images of: (a) measured data, (b) PO simulation of scanned CAD model, and (c) generic CAD model illuminated from the front.

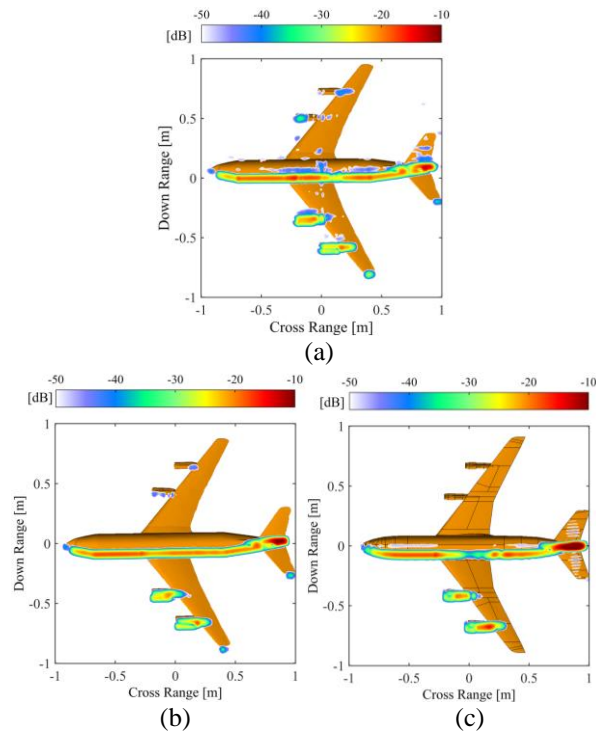


Fig. 7. ISAR images of: (a) measured data, (b) PO simulation of scanned CAD model, and (c) generic CAD model illuminated from the side.

Further analysis of the RCS capabilities of the other asymptotic methods were conducted exclusively with the scanned CAD model to minimize the errors introduced in the radar signature due to geometrical differences between the measured and simulated targets.

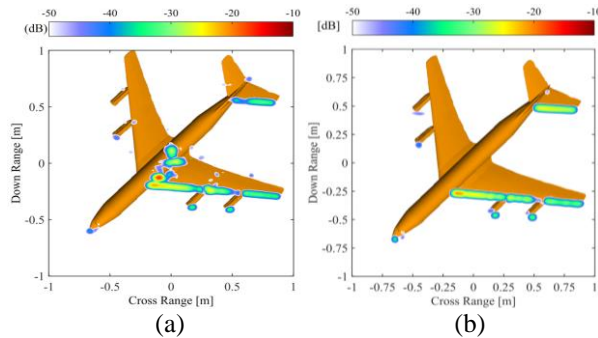


Fig. 8. ISAR images of: (a) measured data, and (b) PO simulation illuminated from 30° to 60° .

III. VALIDATION OF ASYMPTOTIC METHODS

A. RL-GO as implemented in FEKO

RL-GO (FEKO) simulations were performed at 3 GHz and 17 GHz and were validated against measured data. No edge-diffractions were taken into account. The effects of two different mesh types, compatible with this method, on the simulation accuracy were investigated. These meshes included a linear and curvilinear triangular mesh that is available with the FEKO Suite 7.0.2 Feature Update [9, 10]. The RCS of the CAD model, meshed with both types of meshes, was computed with the RL-GO method at both frequencies. One and three interactions were considered. It was found that the RL-GO data using a curvilinear mesh was very inaccurate with multiple interactions and is therefore not shown. The RCS results obtained with the linearly meshed model considering three interactions are provided in Figs. 9 and 10, respectively. The RCS results using both mesh types with one interaction are provided in Figs. 11 and 12, respectively.

It is clear from Figs. 9 and 10 that the RL-GO data using a linear mesh with three interactions follows a similar trend as the measured RCS data. However, large discrepancies are observed between the nose region of the airplane and the broadside reflection (20° to 70°) as well as the broadside reflection and the tail region of the aircraft (110° to 170°).

The simulation accuracy clearly increased significantly with respect to the measured data when only one interaction is considered, especially over the range of 110° to 170° , as seen in Figs. 11 and 12. There is overall excellent agreement between this simulated RCS data and the measured data, especially in the ranges where the RCS values are higher (above -5 dBsm). Some

ranges are still slightly inaccurate, 40° to 60° and 110° to 170° . The RL-GO data of the linearly and curvilinearly meshed models are almost identical. These RL-GO results are also very similar to the PO results shown in Figs. 3 and 5.

Further scattering analysis of the RL-GO method with three interactions is conducted with the linearly meshed target. Scattering analyses are also conducted of the RL-GO method when only one interaction is considered with both mesh types. The same ISAR measurement and simulation setups as described in Section II were implemented, with the illumination from 110° to 170° . Because the RCS calculated with the linearly and curvilinearly meshed model, considering a single interaction, are so similar only the curvilinear data is shown. The three ISAR images are provided in Fig. 13.

It is clear from the ISAR image of the measured data seen in Fig. 13 (a) that the main scattering is produced by the corner reflector created between the trailing edge of the wing and the fuselage, the vertical stabilizer, and the trailing edges of the engines. Most of these main scattering centers are also observed in the RL-GO simulation image in Fig. 13 (b). However, the calculated scattering produced by the engines and the trailing edge of the wing are much higher than the measured data. This explains the larger simulated RCS value over this range in the angular RCS data provided in Figs. 9 and 10. When only one interaction is considered the scattering centers are very similar to the measured data as seen in Fig. 13 (c). The reason for the reduced error in the angular RCS data over this range as seen in Fig. 11 and 12 is due to the less noisy scattering observed between the fuselage and wing of the airplane. The calculated RCS is still slightly higher than the measured data due to the higher scattering produced by the engines and the trailing edge of the wing.

A summary of computational resources required by this method is provided in Table 1.

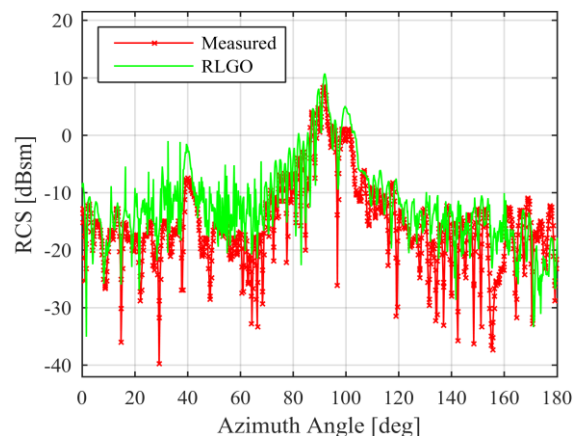


Fig. 9. RCS at 3 GHz measured and simulated in FEKO with RL-GO using a linear mesh considering 3 interactions.

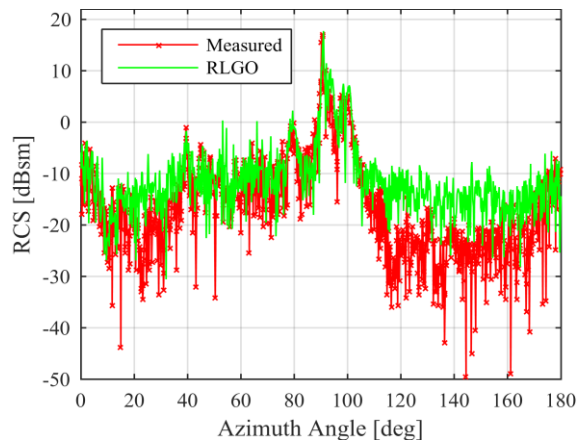


Fig. 10. RCS at 17 GHz measured and simulated in FEKO with RL-GO using a linear mesh considering 3 interactions.

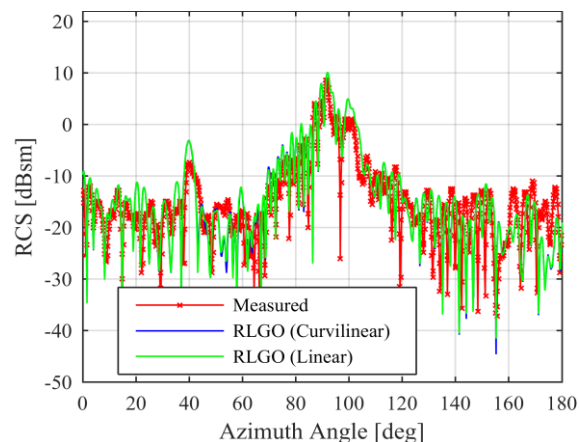


Fig. 11. RCS at 3 GHz measured and simulated in FEKO with RL-GO using linear and curvilinear meshes considering 1 interaction.

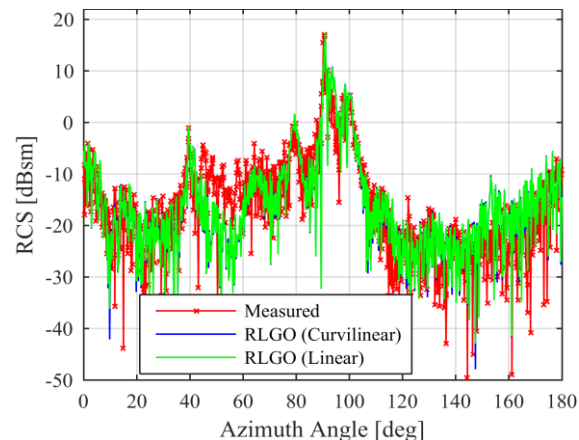


Fig. 12. RCS at 17 GHz measured and simulated in FEKO with RL-GO using linear and curvilinear meshes considering 1 interaction.

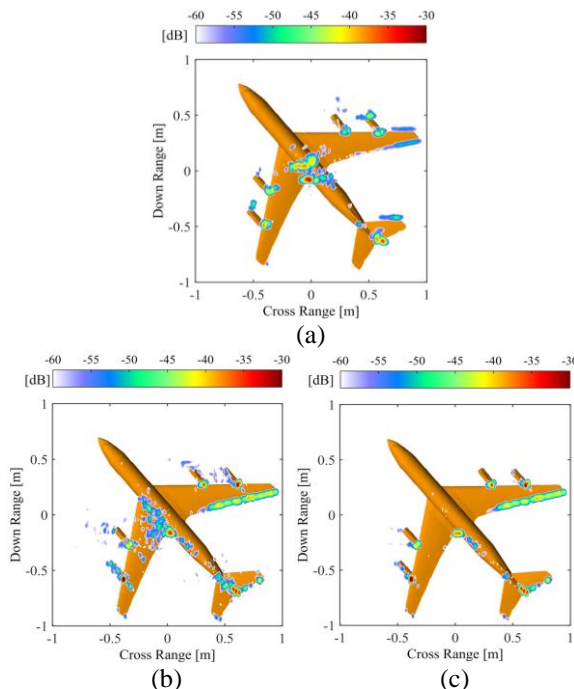


Fig. 13. ISAR images of: (a) measured data, (b) RL-GO simulation using a linear mesh with 3 interactions, and (c) using a curvilinear mesh with 1 interaction, illuminated from 110° to 170° .

B. SBR as implemented in CST MWS

The SBR method implemented in CST MWS 2015 was validated. The ability of this method to calculate the RCS of the airframe was investigated using rays and ray-tubes at 3 GHz and 17 GHz. The optimum number of reflections required, in terms of solution accuracy and execution time, was found to be three. The RCS results are provided in Figs. 14 and 15, respectively.

It is clear from Fig. 14 and Fig. 15 that there is overall excellent agreement between the measurements and the RCS calculated with the SBR method using rays. The RCS calculated with the SBR method using ray-tubes does not compare as well with the measured RCS over the entire azimuth range. Large discrepancies are observed between 40° to 60° where this simulated data is larger than the measured data. In this range, the RCS calculated with the SBR method using rays is slightly lower than the measured data. ISAR images of the measured and SBR simulated data using rays and ray-tubes were generated to examine the disagreements in this range. Figure 16 provides the ISAR images of the measured data, and the SBR simulation using rays, and ray-tubes illuminated from 30° to 60° . A few main scattering points are observed in the image of the measured seen in Fig. 16 (a). These are found at the leading edge of the wing, the juncture between the wing and the fuselage, the engines, the horizontal stabilizer, and the nose of the aircraft. The corner reflector created

between the wing and fuselage is the dominant scatterer over this azimuth range. There is overall excellent agreement between the scattering centers observed in the measured data and the simulated data generated with the SBR method using rays, shown in Fig. 16 (b). The scattering produced by the corner reflector, formed between the wing and the fuselage of the airplane, is slightly lower in this simulated data than in the measured data. This explains the slightly lower simulated RCS values observed in this range seen in Fig. 14 and Fig. 15. The main scattering centers found in the measured data are also observed in the ISAR image produced by the SBR method using ray-tubes, seen in Fig. 16 (c). However, the scattering center produced by the corner reflector, found between the wing and fuselage of the airplane, has a much higher value than the measured data. The simulation data is also noisier, possibly due to cross range smear [11]. This explains why the RCS calculated with this method is higher than the measured data from 40° to 60° .

A summary of computational resources required by this method is provided in Table 1.

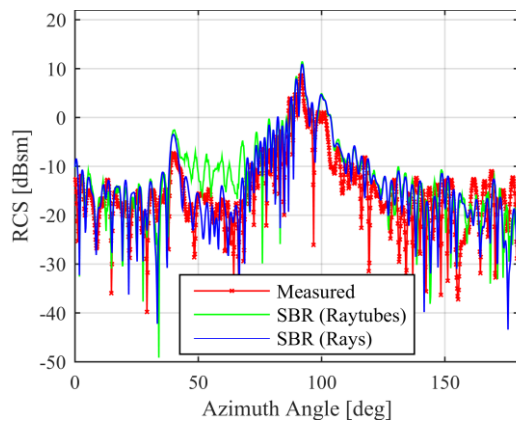


Fig. 14. RCS at 3 GHz measured in the compact range and simulated in CST with SBR using rays and ray-tubes.

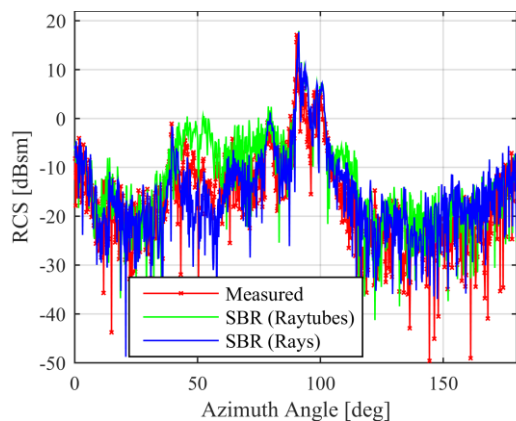


Fig. 15. RCS at 17 GHz measured in the compact range and simulated in CST with SBR using rays and ray-tubes.

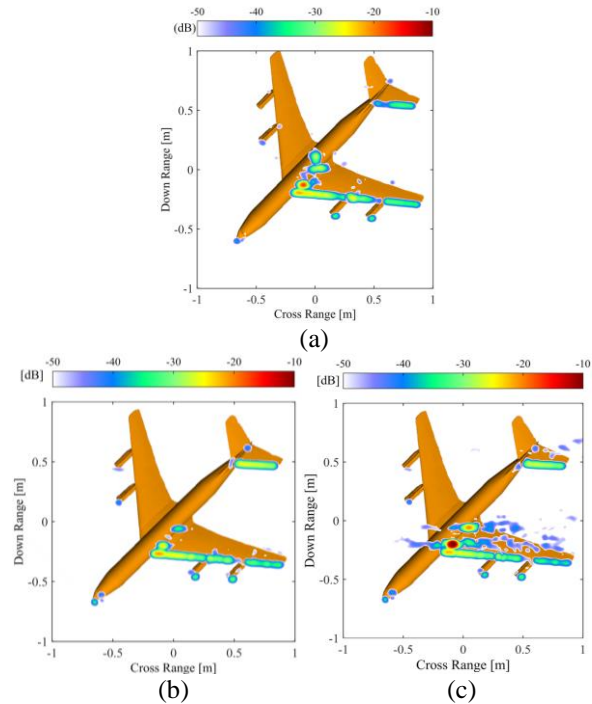


Fig. 16. ISAR images of: (a) measured data, (b) SBR simulation with rays, and (c) with ray-tubes illuminated from 30° to 60° .

Table 1: Summary of computational requirements

Method	Run Time [hrs]	CPU Time [hrs]	RAM [GB]	Mem. Read [GB]	Mem. Write [GB]
RL-GO	2.4	14	2.49	1.58	0.14
SBR rays	0.82	2.52	3.96	6.38	5.97
SBR tubes	1.28	5.53	4.03	6.43	10.10

IV. CONCLUSION

The effect of the geometrical accuracy of the 3D CAD, with respect to the scale model, on the accuracy of the calculated RCS data was investigated. This was done by calculating the RCS of two CAD models and comparing the results with measured RCS data generated in a compact range. A conducting scale model of a Boeing 707, with a maximum electrical length of 106λ , was measured. The two CAD models utilized in this investigation included a laser scanned and a generically constructed CAD model of the target. It was found that the laser scanned CAD model produced more accurately calculated RCS results compared to the measured data than the generic CAD model. Therefore, if measured data is used for validation purposes, the numerical model of the target has to be a very accurate approximation of the measured target. This can be achieved by either laser scanning the physical target or by accurately manufacturing the target from the CAD model specifications. Consequently, the validation of the

asymptotic methods was conducted with the scanned CAD model of the target.

The accuracy with which the RL-GO and SBR asymptotic CEM techniques calculated the RCS of the electrically large complex target was validated. This was done by comparing the simulated RCS results with measured data using RCS plots and ISAR images. Almost all of the simulated RCS data, generated with the various asymptotic methods, followed the same trend as the measurements and had excellent agreement over the ranges where the projected area of the aircraft was large. The accuracy also increased with frequency. Very poor RCS results were obtained when a curvilinear mesh model was simulated with multiple reflections using the RL-GO method in FEKO. However, the accuracy of the RCS results increased when this method was applied to a linearly meshed model. The accuracy of this method increased significantly, with both mesh types, when only one interaction was considered. These results were very similar to the PO results generated with the scanned CAD model. The SBR method as implemented in CST MWS produced accurate RCS results when rays were used and less accurate results when ray-tubes were used.

It was also shown that ISAR imaging provided a handy tool to examine the differences between the measured and simulated radar signatures.

The simulations were performed on a computer with six 3.2 GHz processors and 64 GB RAM. It is clear from Table 1 that the SBR method with rays (CST 2016) was the most time efficient method, and RL-GO (FEKO 14.0.420-552) was the most time demanding. However the RL-GO method (FEKO) was the most memory efficient method whereas the SBR method with ray-tubes (CST) was the least.

ACKNOWLEDGMENT

The authors are grateful for the support received from B. Jacobs for providing the generic CAD model of the target, CST MWS (A. Bhattacharya, A. Ibbotson, and M. Ruetschlin), and FEKO (E. Burger).

REFERENCES

- [1] J. E. Cilliers, J. M. Steyn, J. C. Smit, C. Pienaar, and M. Pienaar, "Considering CAD model accuracy for radar cross section and signature calculations of electrically large complex targets," in *International Radar Conference*, Lille, 2014.
- [2] F. Weinmann, "Ray tracing with PO/PTD for RCS modeling of large complex objects," *IEEE Transactions on Antennas and Propagation*, vol. 54, no. 6, pp. 1797-1806, June 2006.
- [3] J. C. Smit, J. E. Cilliers, and E. H. Burger, "Comparison of MLFMM, PO and SBR for RCS investigations in radar applications," in *IET International Conference on Radar Systems*, Glasgow, 2012.
- [4] I. M. Martin, M. A. Alves, G. G. Peixoto, and M. C. Rezende, "Radar cross section measurements and simulations of a model airplane in the X-band," *PIERS Online*, vol. 5, no. 4, pp. 377-380, 2009.
- [5] B. Jacobs and D. E. Baker, "Validation of a computational electromagnetic model of a Boeing 707 aircraft by comparison to scale model measurements," in *Conference on Antennas and Propagation in Wireless Communications*, Cape Town, 2012.
- [6] C. Pienaar, J. W. Odendaal, J. C. Smit, J. Joubert, and J. E. Cilliers, "RCS results for an electrically large realistic model airframe," Accepted for Publication in the *Applied Computational Electromagnetic Society Express Journal*, 2016.
- [7] FEKO Suite, Altair, South Africa, www.feko.info, 2015.
- [8] CST STUDIO SUITE® 2015, CST AG, Germany, www.cst.com
- [9] U. Jakobus, "Advances in EM simulations," in *Altair Technology Conferences*, Dearborn, MI, USA, 6 May 2015.
- [10] FEKO Altair, "FEKO Suite 7.0.2 Feature Update," 6 May 2015. [Online]. Available: <https://www.feko.info/about-us/News/feko-suite-7.0.2-feature-update/view>. [Accessed Aug. 2015].
- [11] R. Bhalla and H. Ling, "Cross range streaks in ISAR images generated via the shooting-and-bouncing ray technique: Cause and solutions," *IEEE Antennas and Propagation Magazine*, vol. 39, no. 2, pp. 76-80, 1997.